iJRASET
International Journal For Research in Applied Science and Engineering Technology

INTERNATIONAL JOURNAL FOR RESEARCH

IN APPLIED SCIENCE & ENGINEERING TECHNOLOGY

Volume: 13 **Issue:** X **Month of publication:** October 2025

DOI: https://doi.org/10.22214/ijraset.2025.74590

www.ijraset.com

Call: 08813907089 | E-mail ID: ijraset@gmail.com

International Journal for Research in Applied Science & Engineering Technology (IJRASET)
ISSN: 2321-9653; IC Value: 45.98; SJ Impact Factor: 7.538
Volume 13 Issue X Oct 2025- Available at www.ijraset.com

Spectral, Transmittance and Thermal Properties of Nd^{3+} Doped Borophosphate Glasses

S. L. Meena
Ceramic Laboratory, Department of physics, Jai Narain Vyas University, Jodhpur 342001(Raj) India

Abstract: ***Glass of the system :(20-x)P_2O_5: 10ZnO: 10Li_2O: 10CaO: 10Na_2O: 10Sb_2O_3: 10Al_2O_3:10Y_2O_3:10B_2O_3:xNd_2O_3. (where x=1, 1.5,2 mol %) have been prepared by melt-quenching method. The amorphous nature of the glasses was confirmed by X-ray diffraction studies.***

Optical absorption, Excitation, fluorescence, DTA thermogram and Transmittance spectra were recorded at room temperature for all glass samples Slater-Condon parameters F_k (k=2, 4, 6), Lande parameter ξ_{4f} and Racah parameters E^k (k=1, 2, 3) have been computed.

Using these parameters energies and intensities of these bands has been calculated. Judd-Ofelt intensity parameters Ω_λ (λ=2, 4, 6) are evaluated from the intensities of various absorption bands of optical absorption spectra. Using these intensity parameters various radiative properties like spontaneous emission probability (A), branching ratio (β_R), radiative life time (τ_R) and stimulated emission cross–section (σ_p)) of various emission lines have been evaluated.

Keywords: YZLSLAABP Glasses, Thermal and Optical Properties, Judd-Ofelt Theory, Photoluminescence Properties.

I. INTRODUCTION

Among different ceramic glasses, phosphate glasses is attributed to their favorable properties such as high refractive index, high density and high transparency [1-7].Phosphate glass is an extremely promising material for reflecting windows, laser, mechanical sensors and nonlinear applications in optics due to some of its essential characteristic features, such as low phonon energy, low melting temperature and excellent transparency.

They have high thermal stability, high transparency and low dispersion rates [8-14].Phosphate glasses are potentially important host materials for developing rare earth doped optical devices. Phosphate glasses have excellent transparency, good mechanical and thermal stability. Borophosphate glass has low phonon energy, chemical and thermal stability [15,16]. They present superior properties like that high transparency, low melting point, high gain density, high solubility for rare-earth ions and low dispersion. The host matrix compose of ZnO, a glass modifier/glass farmer a heavy metal oxide along with PbO, Li_2O, Sb_2O_3 and B_2O_3.The addition of Na_2O to the glass mixture improves the rare earth ion solubility leading to the possibility of using even higher concentrations of ions [17-19].

The present work reports on the thermal, absorption and emission properties of Nd^{3+} doped yttrium zinc lithium sodalime antimony alumino borophosphate glass. The intensities of the transitions for the rare earth ions have been estimated successfully using the Judd-Ofelt theory, The laser parameters such as radiative probabilities (A), branching ratio (β_R), radiative life time (τ_R) and stimulated emission cross section(σ_p) are evaluated using J.O. intensity parameters (Ω_λ, λ=2,4 and 6).

II. EXPERIMENTAL TECHNIQUES

A. Preparation of Glasses

The following Nd^{3+} doped borophosphate glass samples :(20-x)P_2O_5: 10ZnO: 10Li_2O: 10CaO: 10Na_2O: 10Sb_2O_3: 10Al_2O_3:10Y_2O_3:10B_2O_3: xNd_2O_3. (where *x* =1, 1.5, 2) have been prepared by melt-quenching method. Analytical reagent grade chemical used in the present study consist of P_2O_5, ZnO, Li_2O,CaO, Na_2O,Sb_2O_3,Al_2O_3,Y_2O_3,B_2O_3 and Nd_2O_3. They were thoroughly mixed by using an agate pestle mortar. Then melted at 980˚C by an electrical muffle furnace for 2 hours. After complete melting, the melts were quickly poured in to a preheated stainless steel mould and annealed at temperature of 250˚C for 2 h to remove thermal strains and stresses. Every time fine powder of cerium oxide was used for polishing the samples. The glass samples so prepared were of good optical quality and were transparent. The chemical compositions of the glasses with the name of samples are summarized in Table 1.

Table 1

Sample	Glass composition (mol %)
YZLSLAABP (UD)	**$20P_2O_5$:10ZnO:10Li_2O:10CaO:10Na_2O:10Sb_2O_3:10Al_2O_3:10Y_2O_3:10B_2O_3**
YZLSLAABP ND (1.0)	**$19P_2O_5$:10ZnO:10Li_2O:10CaO:10Na_2O:10Sb_2O_3:10Al_2O_3:10Y_2O_3:10B_2O_3:1Nd_2O_3**
YZLSLAABP ND (1.5)	**18.5 P_2O_5:10ZnO:10Li_2O:10CaO:10Na_2O:10Sb_2O_3:10Al_2O_3:10Y_2O_3:10B_2O_3:1.5Nd_2O_3**
YZLSLAABP ND (2.0)	**$18P_2O_5$:10ZnO:10Li_2O:10CaO:10Na_2O:10Sb_2O_3:10Al_2O_3:10Y_2O_3:10B_2O_3: 2Nd_2O_3**

YZLSLAABP (UD) - Represents undoped Yttrium Zinc Lithium Sodalime Antimony Alumino Borophosphate glass specimen.
YZLSLAABP (ND) - Represents Nd^{3+} doped Yttrium Zinc Lithium Sodalime Antimony Alumino Borophosphate glass specimens.

III. THEORY

A. *Oscillator Strength*

The intensity of spectral lines is expressed in terms of oscillator strengths using the relation [20].

$$f_{expt.} = 4.318 \times 10^{-9} \int \varepsilon(\nu)\, d\nu \qquad (1)$$

where, $\varepsilon(\nu)$ is molar absorption coefficient at a given energy ν (cm^{-1}), to be evaluated from Beer–Lambert law.
Under Gaussian Approximation, using Beer–Lambert law, the observed oscillator strengths of the absorption bands have been experimentally calculated [21], using the modified relation:

$$P_m = 4.6 \times 10^{-9} \times \frac{1}{cl} \log \frac{I_0}{I} \times \Delta\upsilon_{1/2} \qquad (2)$$

Where c is the molar concentration of the absorbing ion per unit volume, I is the optical path length, $\log I_0/I$ is optical density and $\Delta\upsilon_{1/2}$ is half band width.

B. *Judd-Ofelt Intensity Parameters*

According to Judd [22] and Ofelt [23] theory, independently derived expression for the oscillator strength of the induced forced electric dipole transitions between an initial J manifold $|4f^N (S, L) J\rangle$ level and the terminal J' manifold $|4f^N (S', L') J'\rangle$ is given by:

$$\frac{8\Pi^2 mc\bar{\upsilon}}{3h(2J+1)} \frac{1}{n}\left[\frac{(n^2+2)^2}{9}\right] \times S(J, J') \qquad (3)$$

Where,

the line strength S (J, J') is given by the equation

$$S(J, J') = e^2 \sum_{\lambda=2,4,6} \Omega_\lambda \langle 4f^N (S, L) J \| U^{(\lambda)} \| 4f^N (S', L') J' \rangle^2 \qquad (4)$$

In the above equation m is the mass of an electron, c is the velocity of light, ν is the wave number of the transition, h is Planck's constant, n is the refractive index, J and J' are the total angular momentum of the initial and final level respectively, Ω_λ (λ=2,4and 6) are known as Judd-Ofelt intensity parameters.

C. *Radiative Properties*

The Ω_λ parameters obtained using the absorption spectral results have been used to predict radiative properties such as spontaneous emission probability (A) and radiative life time (τ_R), and laser parameters like fluorescence branching ratio (β_R) and stimulated emission cross section (σ_p).

The spontaneous emission probability from initial manifold $|4f^N (S', L') J'\rangle$ to a final manifold $|4f^N (S, L) J\rangle$ is given by:

$$A[(S', L') J'; (S, L) J] = \frac{64\pi^2\nu^3}{3h(2J'+1)}\left[\frac{n(n^2+2)^2}{9}\right] \times S(J', \bar{J}) \qquad (5)$$

Where, $S(J', J) = e^2 [\Omega_2 \| U^{(2)} \|^2 + \Omega_4 \| U^{(4)} \|^2 + \Omega_6 \| U^{(6)} \|^2]$

The fluorescence branching ratio for the transitions originating from a specific initial manifold $|4f^N (S', L') J'>$ to a final many fold $|4f^N (S, L) J >$ is given by

$$\beta [(S', L') J'; (S, L) J] = \frac{A[(S' L)]}{\sum_{S L J} A[(S' L') J' (\bar{S} L)]} \quad (6)$$

The radiative life time is given by

$$\tau_{rad} = \sum_{S L J} A[(S', L') J'; (S, L)] = A^{-1}_{Total} \quad (7)$$

Where, the sum is over all possible terminal manifolds. The stimulated emission cross -section for a transition from an initial manifold $|4f^N (S', L') J'>$ to a final manifold $|4f^N (S, L) J >|$ is expressed as

$$\sigma_p(\lambda_p) = \left[\frac{\lambda_p^4}{8\pi c n^2 \Delta\lambda_{eff}}\right] \times A[(S', L') J'; (\bar{S}, \bar{L}) \bar{J}] \quad (8)$$

Where, λ_p the peak fluorescence wavelength of the emission band and $\Delta\lambda_{eff}$ is the effective fluorescence line width.

D. Nephelauxetic Ratio (β) and Bonding Parameter ($b^{1/2}$)

The nature of the R-O bond is known by the Nephelauxetic Ratio (β') and Bonding Parameters ($b^{1/2}$), which are computed by using following formulae [24,25]. The Nephelauxetic Ratio is given by

$$\beta' = \frac{\nu_g}{\nu_a} \quad (9)$$

where, ν_a and ν_g refer to the energies of the corresponding transition in the glass and free ion, respectively. The values of bonding parameter $b^{1/2}$ are given by

$$b^{1/2} = \left[\frac{1-\beta'}{2}\right]^{1/2} \quad (10)$$

IV. RESULT AND DISCUSSION

A. XRD Measurement

Figure 1 presents the XRD pattern of the samples shows no sharp Bragg's peak, but only a broad diffuse hump around low angle region. This is the clear indication of amorphous nature within the resolution limit of XRD instrument.

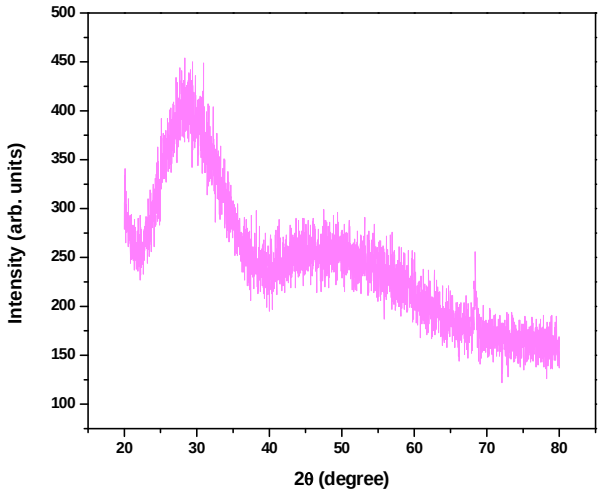

Fig.1: X-ray diffraction pattern of YZLSLAABP ND (1.0) glass.

B. Transmittance Spectrum

The Transmittance spectrum of Nd^{3+}doped in yttrium zinc lithium sodalime antimony alumino borophosphate glass is shown in Figure 2.

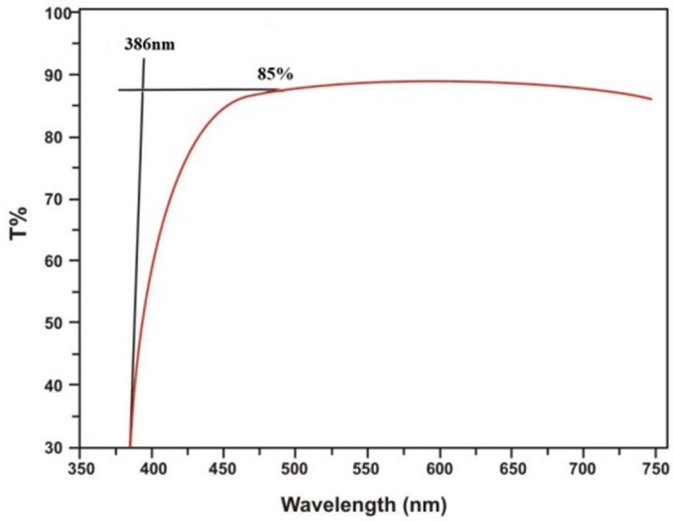

Fig.2: Transmittance spectrum of YZLSLAABP ND (1.0) glass.

C. Thermal Property

Differential thermal analysis checks the heat absorbed by glass samples during heating or cooling. Fig. 3 depicts the DTA thermogram of powdered YZLSLAABP sample. The glass transition temperature (T_g), onset crystallization temperature (T_c), crystallization temperature (T_p), melting temperature(T_m), thermal stability (T_s),Balaji Parameter (B_P), Hurbe's criterion (H_R) and reduced glass transition temperature (T_{rg}) were calculated. Shankar's parameter also calculated by using eq. (12). All the determined thermal parameters are given in table 2.

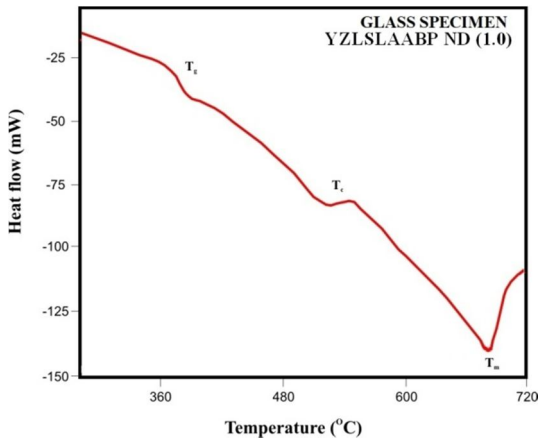

Fig.3: DTA curve of YZLSLAABP ND (1.0) glass.

Table 2. Thermal parameters determined from the DTA traces of YZLSLAABP ND glasses.

Sample Name	T_g(^{0}C)	T_c(^{0}C)	T_p(^{0}C)	T_m(^{0}C)	T_s(^{0}C)	B_P(^{0}C)	H_R(^{0}C)	K_S(^{0}C)	T_{rg}(^{0}C)
YZLSLAABP ND (1.0)	375	509	546	687	134	3.622	0.753	34.719	0.546
YZLSLAABP ND (1.5)	377	510	548	680	133	3.500	0.782	33.250	0.554
YZLSLAABP ND (2.0)	380	512	556	691	132	3.000	0.737	34.194	0.550

The thermal stability of the glass samples can be calculated by difference between onset crystallization temperature and transition temperature [26].

Thermal stability (T_s) =T_c-T_g (11)

Balaji Parameter can be calculated using [27].

Balaji Parameter (B_P) = [(T_c-T_g)/(T_p-T_c)] (12)

Hruby's criterion is calculated using the Hurby's relation [28].

Hruby's criterion (H_R) = [(T_p-T_c)/(T_m-T_c)] (13)

Reduced glass transition temperature is given as [29].

Reduced glass transition temperature (T_{rg}) =T_g/T_m (14)

Thermal Parameter is given as [30].

K_S= [(T_m-T_c) (T_c-T_g)/T_m] (15)

D. Absorption Spectra

The absorption spectra of YZLSLAABP ND (1.0) glass, consists of absorption bands corresponding to the absorptions from the ground state $^4I_{9/2}$ of Nd^{3+} ions. Nine absorption bands have been observed from the ground state $^4I_{9/2}$ to excited states $^4F_{3/2}$, $^4F_{5/2}$, $^4F_{7/2}$, $^4F_{9/2}$, $^2H_{11/2}$, $^4G_{5/2}$, $^4G_{7/2}$, $^4G_{9/2}$, and $^2G_{9/2}$ for Nd^{3+} doped YZLSLAABP ND (1.0) glass.

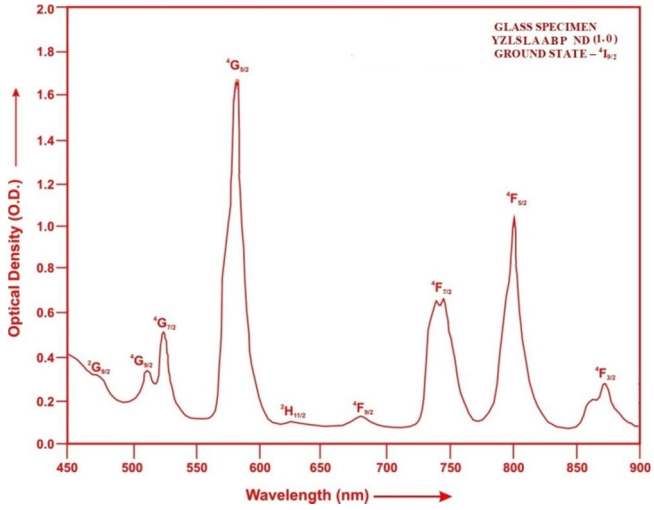

Fig.4: Absorption spectra of YZLSLAABP ND (1.0) glass.

The experimental and calculated oscillator strength for Nd^{3+} ions in YZLSLAABP glasses are given in **Table 3.**

Table 3. Measured and calculated oscillator strength ($P^m \times 10^{+6}$) of Nd^{3+} ions in YZLSLAABP glasses.

Energy level from $^4I_{9/2}$	Glass YZLSLAABP ND(1.0)		Glass YZLSLAABP ND(1.5)		Glass YZLSLAABP ND(2.0)	
	$P_{exp.}$	$P_{cal.}$	$P_{exp.}$	$P_{cal.}$	$P_{exp.}$	$P_{cal.}$
$^4F_{3/2}$	3.52	3.48	3.47	3.47	3.42	3.45
$^4F_{5/2}$	8.42	8.42	8.39	8.38	8.35	8.35
$^4F_{7/2}$	9.54	9.85	9.5	9.83	9.45	9.81
$^4F_{9/2}$	0.66	0.52	0.64	0.52	0.61	0.52
$^2H_{11/2}$	0.29	0.15	0.27	0.15	0.25	0.15
$^4G_{5/2}$	25.45	25.70	24.36	24.63	23.45	23.74
$^4G_{7/2}$	4.25	5.08	4.2	5.00	4.16	4.93
$^4G_{9/2}$	2.25	2.19	2.21	2.18	2.17	2.17
$^2G_{9/2}$	0.95	2.78	0.93	2.77	0.90	2.76
r.m.s.deviation	0.7681		0.6862		0.6896	

Table4. Computed values of Slater-Condon, Lande, Racah, nephelauexetic ratio and bonding parameter for Nd^{3+} doped YZLSLAABP glass specimens.

Parameter	Free ion	YZLSLAABP ND(1.0)	YZLSLAABP ND(1.5)	YZLSLAABP ND(2.0)
$F_2(cm^{-1})$	331.16	324.58	324.59	324.59
$F_4(cm^{-1})$	50.71	50.72	50.72	50.72
$F_6(cm^{-1})$	5.154	5.038	5.041	5.039
$\xi_{4f}(cm^{-1})$	884.0	882.73	882.72	882.78
$E^1(cm^{-1})$	5024.0	4947.12	4947.19	494.72
$E^2(cm^{-1})$	23.90	23.08	23.08	23.08
$E^3(cm^{-1})$	497.0	489.58	489.59	489.57
F_4/F_2	0.1531	0.1563	0.1563	0.1562
F_6/F_2	0.0155	0.0155	0.0155	0.0155
E^1/E^3	10.1086	10.1048	10.1047	10.1052
E^2/E^3	0.0481	0.0471	0.0471	0.0471
β'		0.995807	0.995817	0.995822
$b^{1/2}$		0.04578	0.04573	0.04571

The values of Judd-Ofelt intensity parameters are given in **Table 5**.

Table 5. Judd-Ofelt intensity parameters for Nd^{3+} doped YZLSLAABP glass specimens.

Glass Specimen	$\Omega_2(pm^2)$	$\Omega_4(pm^2)$	$\Omega_6(pm^2)$	Ω_4/Ω_6
YZLSLAABP ND(1.0)	2.919	7.396	3.623	2.041
YZLSLAABP ND(1.5)	2.572	7.361	3.616	2.036
YZLSLAABP ND(2.0)	2.288	7.326	3.604	2.033

E. Excitation Spectrum

The Excitation spectra of Nd^{3+}doped YZLSLAABP ND (1.0) glass specimen has been presented in Figure 5 in terms of Excitation Intensity versus wavelength. The excitation spectrum was recorded in the spectral region 700–1000 nm fluorescence at 1065nm having different excitation band centred at 808 nm and 887 nm are attributed to the ($^4I_{9/2}\rightarrow{}^4F_{5/2}$) and ($^4I_{9/2}\rightarrow{}^4F_{3/2}$) transitions, respectively. The highest absorption level is ($^4I_{9/2}\rightarrow{}^4F_{5/2}$) and is at 808 nm. So this is to be chosen for excitation wavelength.

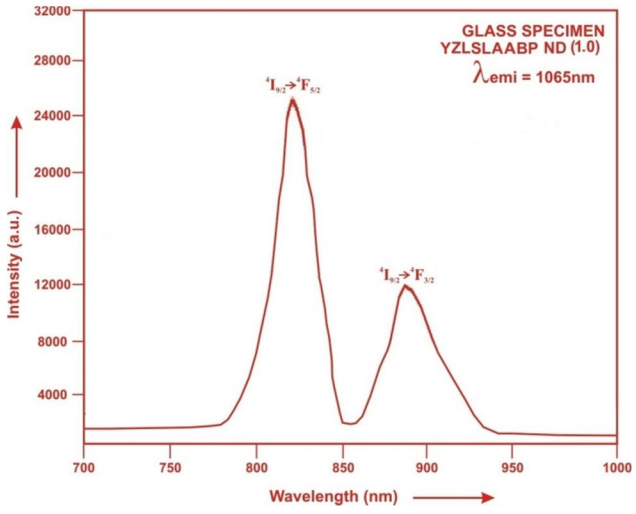

Fig.5: Excitation spectra of YZLSLAABP ND (1.0) glass.

F. Fluorescence Spectrum

The fluorescence spectrum of Nd^{3+}doped in yttrium zinc lithium sodalime antimony alumino borophosphate is shown in Figure 6. There are six broad bands ($^4G_{7/2}\rightarrow{}^4I_{9/2}$), ($^4G_{7/2}\rightarrow{}^4I_{11/2}$), ($^4F_{3/2}\rightarrow{}^4I_{9/2}$) ($^4F_{3/2}\rightarrow{}^4I_{11/2}$), ($^4F_{3/2}\rightarrow{}^4I_{13/2}$) and ($^4F_{3/2}\rightarrow{}^4I_{15/2}$) respectively for glass specimens.

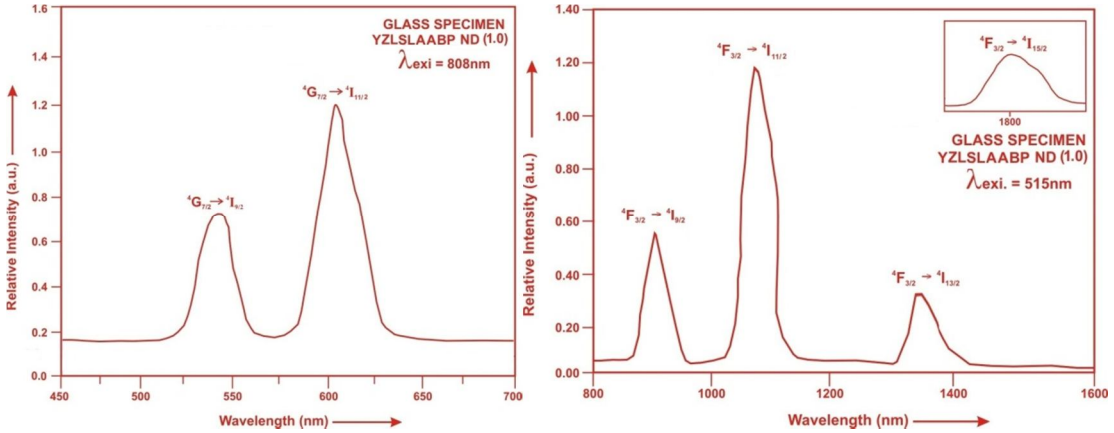

Fig.6: Fluorescence spectrum of YZLSLAABP ND (1.0) glass.

The wavelengths of these bands along with their assignments are given in **Table 6**.

Table 6. Emission peak wave lengths (λ_p), radiative transition probability (A_{rad}), branching ratio (β_R), stimulated emission crosssection (σ_p), and radiative life time (τ_R) for various transitions in Nd^{3+} doped YZLSLAABP glasses.

Transition		YZLSLAABP ND(1.0)				YZLSLAABP ND (1.5)				YZLSLAABP ND (2.0)			
	λ_{max} (nm)	$A_{rad}(s^{-1})$	β	σ_p (10^{-20} cm^2)	τ_R(μs)	$A_{rad}(s^{-1})$	β	σ_p (10^{-20} cm^2)	τ_R (μs)	$A_{rad}(s^{-1})$	β	σ_p (10^{-20} cm^2)	τ_R (10^{-20} cm^2)
$^4G_{7/2}\rightarrow{}^4I_{9/2}$	532	2994.67	0.4131	0.446	137.95	2942.23	0.4181	0.458	142.13	2897.79	0.4226	0.471	145.82
$^4G_{7/2}\rightarrow{}^4I_{11/2}$	595	3007.65	0.4149	1.174		2849.22	0.4050	1.169		2718.41	0.3964	1.144	
$^4F_{3/2}\rightarrow{}^4I_{9/2}$	905	729.86	0.1007	0.726		728.08	0.1035	0.741		726.19	0.1059	0.766	
$^4F_{3/2}\rightarrow{}^4I_{11/2}$	1075	440.69	0.0608	2.065		440.21	0.0626	2.151		439.36	0.0641	2.278	
$^4F_{3/2}\rightarrow{}^4I_{13/2}$	1320	74.28	0.0102	0.423		74.29	0.0106	0.442		74.19	0.0108	0.457	
$^4F_{3/2}\rightarrow{}^4I_{15/2}$	1800	1.78	0.0002	0.026		1.78	0.0003	0.026		1.77	0.0003	0.027	

V. CONCLUSION

In the present study, the glass samples of composition :$(20-x)P_2O_5$: $10ZnO$: $10Li_2O$: $10CaO$: $10Na_2O$: $10Sb_2O_3$: $10Al_2O_3$:$10Y_2O_3$:$10B_2O_3$: xNd_2O_3. (where x =1, 1.5, 2 mol %) have been prepared by melt-quenching method. The stimulated emission cross section (σ_p) has highest value for the transition ($^4F_{3/2}\rightarrow{}^4I_{11/2}$) in all the glass specimens doped with Nd^{3+} ion. This shows that ($^4F_{3/2}\rightarrow{}^4I_{11/2}$) transition is most probable transition. Large Balaji and thermal parameters shows that the prepared glass samples are useful for Thermionic Applications.

REFERENCES

[1] Meena,S.L.(2025).Spectral, Transmittance and Upconversion Properties of Pr^{3+} Doped Bismuth Borate Glasses,IOSR-Appl.Phys.17,20-27.
[2] Matous,I.S.,Balzaretti,N.M.(2024).Effect of mixed alkali ions on the structural and spectroscopic properties of Nd^{3+} doped silicate glasses,Results Mat.21,100517.

[3] Asyikin,A.S.,Halimah,M.K.,Latif,A.A.,Faznny,M.F.Nazrin,S.N.(2020).Physical,structural and optical properties of bio-silica borotellurite glass system doped with samarium oxide nanoparticles,J.Non-Cryst.Solids,529,119777
[4] Kashif,I.,Ratep,A.(2023).Influence of dysprosium oxide on physical and optical characteristics of zinc boro-tellurite glasses for optoelectronic device application,Res.Opt.11,100401.
[5] Klimesz,B., Romanowski,W.R.,Lisiecki,R.(2024)Spectroscopic and Thermographic qualities of praseodymium doped oxyfluorotellurite glasses,Molecules,29,3041.
[6] Sigh,H.,Singh,D.,Singh,S.P.(2025).Er^{3+},Nd^{3+},Tm^{3+}:Upconversion in lead borophosphate glasses for visible emission,35:5135-5157.
[7] Kaur, R.B.R.,Kumar,A.(2021).Physical,optical,structural and thermoluminescence behavior of borosilicate glass doped with trivalent neodymium ions,Opt.Mat.117,1-13
[8] Meena,S.L.(2024).Spectral and Luminescence Study of Er^{3+} Doped Phosphate Glasses for the Development of 1.5 μm Broadband Amplifier, IOSR Appl.Phys.16,35-41.
[9] Iscoa,P.L.,Ojha,N.,Aryal,U.,Pugliese,D.,Boetti,N.G.,Milanese,D.,Petit,L.(2019).Spectroscopic Properties of Er^{3+} doped particle containing phosphate glasses fabricated using the direct doping method,Materials,12,129,1-12
[10] Deepa, A. V., murygasen, Priya, Muralimanohar, P., Sathyamoorthy, K.and Vinothkumar, P.(2019). A comparison on the structural and optical properties of different rare earth doped phosphate glass, Optik, 181,361-367
[11] Maheshwari, K., Rao, A. S.(2022). Photoluminescence downshifting studies of thermally stable Dy^{3+} ions doped phosphate glasses for photonic device applications. Opt. Mater.129,112518.
[12] Jlassi, I.; Doddoji, R.(2024). Structural, UV light-excitable luminescence and warm white light generation of dysprosium ionactivated zinc leadfluoride sodium phosphate glasses. J. Mater. Sci. Mater. Electron. 35,748.
[13] Linganna, K.,Haritha, P., Venkata Krishnaiah, K.,Venkatramu, V., Jayasankar, C. K.(2014). Optical and luminescence properties of Dy^{3+} ions in K−Sr−Al phosphate glasses for yellow laser applications. Appl. Phys. B,117, 75−84.
[14] Jimenez,J.A.,Hedge,V.,Viswanath,C.S.D.,Amesimenu,R.(2024). Insights into the Structural, Thermal/Dilatometric, and Optical Properties of Dy^{3+}-Doped Phosphate Glasses for Lighting Applications, ACS Phys. Chem Au, 4, 720−735.
[15] Meena,S.L.(2023). Spectral and Raman Analysis of Er^{3+} Doped Ytterbium Zinc Lithium Sodalime Magnesium Borophosphate Glasses, Int. J. Innov. Res. Sci. Eng.Tech.12, 10915-10924.
[16] Kumar,M.V.,Marimuthu,K.(2015).Structural and luminescence properties of Dy^{3+} doped oxyfluoro-borophosphate glasses for lasing materials and white LEDs J. Alloys-Compds.629,230-241.
[17] Pal, M., Roy, B.and Pal, M. (2011). Structural characterization of borate glasses containing zinc and manganese oxide. J.Mod. Physics, 2, 1062-66.
[18] Dahiya, M.S., Khasa,S. and Agarwal,A. (2015).Physical, thermal, structural and optical absorption studies of vanadyl doped magnesium oxy-chloride bismo-borate glasses . Journal of Asian Ceramic Societies 3, 206–211.
[19] Parandamaiah,M.(2015). Dy $^{3+}$doped Lithium Sodium Bismuth Borate Glasses for Yellow Luminescent Photonic Applications, 5,126-131.
[20] Meena,S.L.(2024).Spectral and Thermal properties of Tm^{3+}doped in zinc lithium tungsten antimonyborophosphate glasses, IOSR Appl.Phys.16,10-15.
[21] Meena,S.L.(2025).Spectral and Thermal properties of Eu^{3+} doped ytteriumzinc lithium alumina tungsten potassiumniobatebismuth borate glasses with low Hruby's criterion, IOSR Appl.Phys.17,48-54.
[22] Judd, B.R.(1962).Optical absorption intensities of rare earth ions,Phys.Rev.127,750-761.
[23] Ofelt, G.S. (1962). Intensities of crystal spectra of rare earth Ions, Chem.Phys37, 511-520.
[24] Ahmad,A.U.,Hashim,S.,Goshal,S.K.(2019).Optical traits of neodymium-doped new types of borate glasses: Judd-Ofelt analysis,Optik,199,163515.
[25] Meena,S.L.(2020). Spectroscopic properties of Tm^{3+} doped in zinc lithium alumino antimony borophosphate glasses,IOSR Appl.Phys.12,36-41
[26] Shwetha,M.,Eraiah,B.(2019).Influence of Er^{3+} ions on the physical,structural,optical and thermal properties of ZnO-Li_2O-P_2O_5 glasses,Appl.Phys.A,125:221
[27] Meena,S.L.(2025). Spectral, Thermal and Raman Analysis Of Ho^{3+}Doped Borophosphate Glasses With Large Balaji Parameter,IOSR Appl.Phys.17,24-31.
[28] Meena,S.L.(2025).Spectral and Thermal properties of Eu^{3+} doped ytteriumzinc lithium alumina tungsten potassiumniobatebismuth borate blasses with low Hruby's criterion, IOSR Appl.Phys.17,48-54.
[29] Meena,S.L.(2024).Spectral, Thermal and FTIR analysis of Pr^{3+}doped in Zinc Lithium Sodium Lead Tungsten Aluminophosphate glasses, Int. J. Innov. Res. Sci. Eng. Tech.13,235-244.
[30] Meena,S.L.(2025).Spectral, Thermal and Raman Analysis of Dy^{3+} Doped Borosilicate Glasses with Large Thermal Stability Parameter,Int.J.Eng.Sci.Inv.14,11-18.

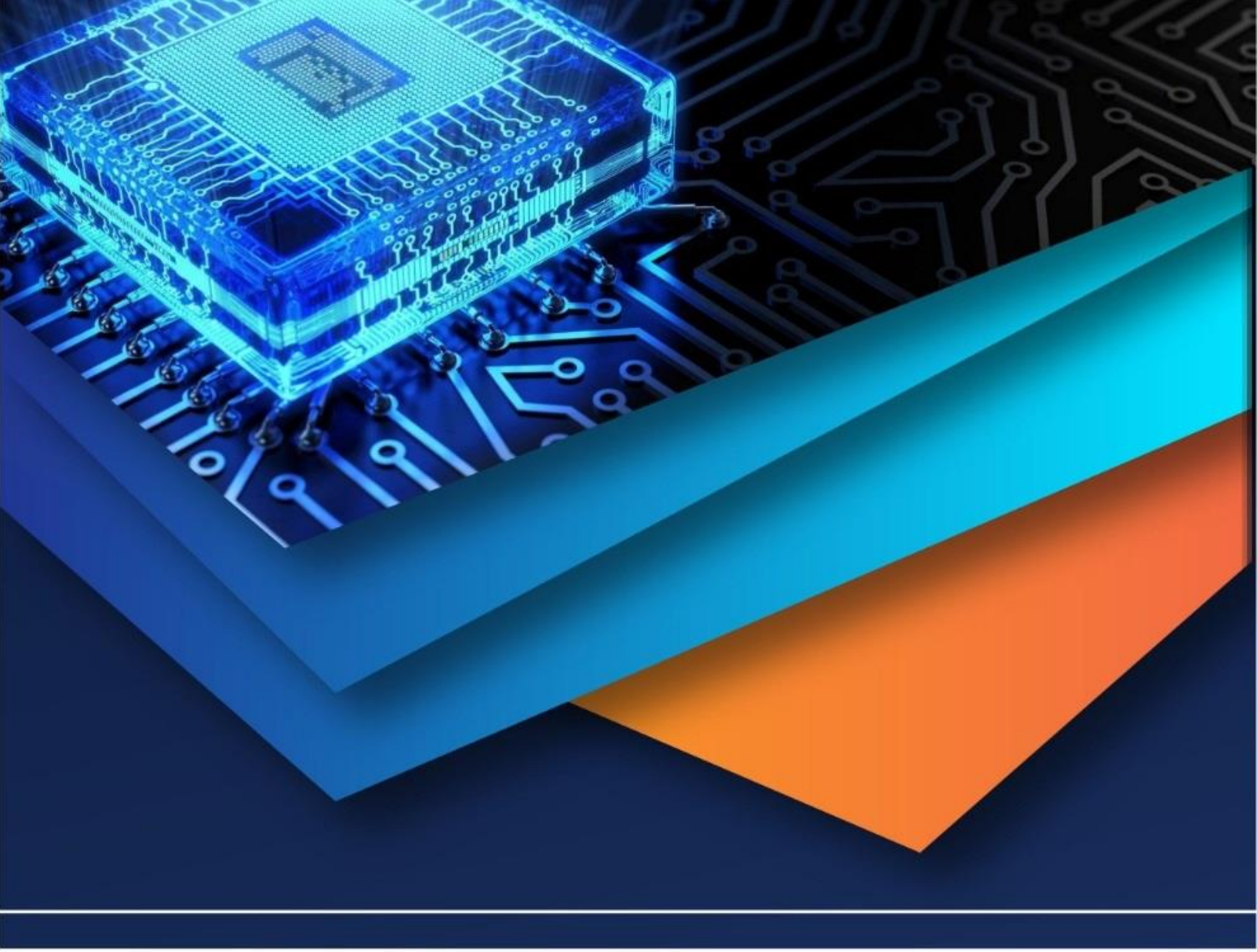

10.22214/IJRASET

45.98

IMPACT FACTOR: 7.129

IMPACT FACTOR: 7.429

INTERNATIONAL JOURNAL FOR RESEARCH

IN APPLIED SCIENCE & ENGINEERING TECHNOLOGY